Research in Pharmaceutical Sciences, February 2015; 10(1): 17-33
Received: Feb 2014
Accepted: Apr 2014

School of Pharmacy & Pharmaceutical Sciences
Isfahan University of Medical Sciences

Original Article

Formulation and optimization of solid lipid nanoparticle formulation for pulmonary delivery of budesonide using Taguchi and Box-Behnken design

J. Emami[1,*], H. Mohiti[1], H. Hamishehkar[2], and J. Varshosaz[3]

[1]*Department of Pharmaceutics and Isfahan Pharmaceutical Research Center, School of Pharmacy and Pharmaceutical Sciences, Isfahan University of Medical Sciences, Isfahan, I.R. Iran.*
[2]*Pharmaceutical Technology Laboratory, Drug Applied Research Center, Tabriz University of Medical Sciences, Tabriz, I.R. Iran.*
[3]*Department of Pharmaceutics and Novel Drug Delivery Systems Research Center, School of Pharmacy and Pharmaceutical Sciences, Isfahan University of Medical Sciences, Isfahan, I.R. Iran.*

Abstract

Budesonide is a potent non-halogenated corticosteroid with high anti-inflammatory effects. The lungs are an attractive route for non-invasive drug delivery with advantages for both systemic and local applications. The aim of the present study was to develop, characterize and optimize a solid lipid nanoparticle system to deliver budesonide to the lungs. Budesonide-loaded solid lipid nanoparticles were prepared by the emulsification-solvent diffusion method. The impact of various processing variables including surfactant type and concentration, lipid content organic and aqueous volume, and sonication time were assessed on the particle size, zeta potential, entrapment efficiency, loading percent and mean dissolution time. Taguchi design with 12 formulations along with Box-Behnken design with 17 formulations was developed. The impact of each factor upon the eventual responses was evaluated, and the optimized formulation was finally selected. The size and morphology of the prepared nanoparticles were studied using scanning electron microscope. Based on the optimization made by Design Expert 7® software, a formulation made of glycerol monostearate, 1.2 % polyvinyl alcohol (PVA), weight ratio of lipid/drug of 10 and sonication time of 90 s was selected. Particle size, zeta potential, entrapment efficiency, loading percent, and mean dissolution time of adopted formulation were predicted and confirmed to be 218.2 ± 6.6 nm, -26.7 ± 1.9 mV, 92.5 ± 0.52 %, 5.8 ± 0.3 %, and 10.4 ± 0.29 h, respectively. Since the preparation and evaluation of the selected formulation within the laboratory yielded acceptable results with low error percent, the modeling and optimization was justified. The optimized formulation co-spray dried with lactose (hybrid microparticles) displayed desirable fine particle fraction, mass median aerodynamic diameter (MMAD), and geometric standard deviation of 49.5%, 2.06 μm, and 2.98 μm; respectively. Our results provide fundamental data for the application of SLNs in pulmonary delivery system of budesonide.

Keywords: Solid lipid nanoparticle; Budesonide; Pulmonary delivery; Box- Behnken; Taguchi design

INTRODUCTION

Amodiaquine is used in the prophylaxis and treatment of malaria especially against chloroquine-resistant isolates of *Plasmodium falciparum* (1). However, the clinical use of this drug is associated with hepato-toxicity (2,3). The exact mechanism of amodiaquine-induced hepatotoxicity is not clear yet, but this adverse effect has been attributed to the bioactivation of the drug to a quinoneimine metabolite (4). Oxidative stress has been suggested to be involved in the development of amodiaquine-induced hepatotoxicity due to the ability of redox cycling induction by the quinoneimine metabolite of amodiaquine (5,6). Such reactive metabolites can irreversibly bind to proteins, which might lead to toxicity by disrupting the cell functions. Since reactive intermediates are formed during amodiaquine metabolism, amodiaquine toxicity mechanism could

*Corresponding author: J. Emami
Tel: 0098 31 37922586, Fax: 0098 31 36680011
Email: emami@pharm.mui.ac.ir

involve protein carbonylation. Lipid peroxidation is a consequence of oxidative stress (7). It has been shown that lipid peroxidation occurred after amodiaquine treatment (8,9). Glutathione reservoirs seems to have critical role in preventing amodiaquine hepatotoxicity (10). Hence, in present study, amodiaquine-induced cytotoxicity was evaluated in intact and glutathione-depleted hepatocytes to elucidate the role of glutathione reservoirs in the toxicity induced by this drug.

Taurine, a conditionally essential amino acid, has several physiological roles (11). There are many reports on taurine protective effects against different chemicals-induced hepatotoxicity (12-14). It has been reported that this amino acid could act as an antioxidant in biological systems (15). Hence, the protective effects of taurine could be due to the antioxidant capability of this amino acid. Being an antioxidant, it has also the ability to scavenge the reactive oxygen species; attenuate lipid peroxidation, and consequently stabilize the biological membranes (16,17).
Considering the previously reported hepatotoxicity associated with amodiaquine, it becomes imperative to study on effective protective agents, which could reduce liver injury caused by this drug. Since taurine has shown protective properties such as antioxidative (18), lipid peroxidation attenuating (19), and/or cellular membrane stabilizing (20) , this study attempted to evaluate the potential protective effects of this amino acid against amodiaquine-induced cellular injury. N-acetyl cysteine (NAC) was used as a thiol containing protective agent since its hepatoprotective properties has been proven in many investigations (21-23). Cell death, reactive oxygen species (ROS) formation, lipid peroxidation, protein carbonylation, and mitochondrial depolarization were assessed as toxicity markers after amodiaquine treatment and the protective effects of taurine and/or N-acetyl cysteine were evaluated.

MATERIALS AND METHODS

Materials

Budesonide was provided by AstraZeneca (UK). Glycerin monostearate (GMS) and cholesterol purchased from Merck (Germany) were used as the lipid materials for the preparation of SLNs. Poloxamer 188 (PLX) and PVA (80% hydrolysis degree and molecular mass 9,000–10,000 g/mol) procured from Sigma Aldrich (Germany) were employed as the emulsifier. Double-distilled water was used for all solutions and dilutions. All the other reagents were of analytical grade.

Preparation of budesonide-loaded solid lipid nanoparticles

Budesonide-loaded SLNs were prepared by the emulsification-solvent diffusion method. Briefly, fixed amount of budesonide (2 mg) and different quantities of lipid materials were dissolved in 2 ml acetone/ethanol mixture at various proportions (Table 1). The aqueous phase contained different percentages of PVA or PLX in different volumes. Both phases were pre-heated to 70 °C and then the organic phase was dripped in to the aqueous phase with a syringe. The mixture was stirred for 30 min to remove acetone and ethanol. The suspension was then sonicated using a microtip probe sonicator set at 50 W energy output (HD 3200, Bandeline, Germany) during various times to obtain Bud-SLNs (Table 1).

Experimental design

The experiment was designed in two separate phases. In the first step, a Taguchi design with seven variables at two different levels was used to determine the factors affecting particle size (PS), zeta potential (ZP), entrapment efficiency (EF), loading percent (LP), and mean release time (MRT) (Table 1). The second step was devoted to further characterization of the significant factors selected from Taguchi design as well as the determination of an optimum formulation using response surface modeling (RSM) (Box-Behnken design).

Some of the variables from Taguchi design were found almost insignificant and were, therefore, excluded from the Box-Behnken design. In the next step, using the Design Expert 7® software, a Box-Behnken design was performed to investigate the further contribution of each factor which was found to be significant in Taguchi design. The variables, levels, and the formulations that resulted using Box-Behnken design are listed in Table 2.

Table 1. Designed formulations for the evaluation of budesonide nanoparticles using Taguchi design.

Formulations	Lipid type	Surfactant type	Surfactant content (%)	lipid/drug	Acetone /ethanol (V/V)	Organic phase/ aqueous phase (V/V)	Sonication time (S)
F1	CHOL	PVA	1	10	1:1	2:25	60
F2	CHOL	PVA	1	10	1:1	2:50	120
F3	CHOL	PVA	2	30	1.5:0.5	2:25	60
F4	CHOL	PLX 188	1	30	1.5:0.5	2:25	120
F5	CHOL	PLX 188	2	10	1.5:0.5	2:50	60
F6	CHOL	PLX 188	2	30	1:1	2:50	120
F7	GMS	PVA	2	30	1:1	2:25	120
F8	GMS	PVA	2	10	1.5:0.5	2:50	120
F9	GMS	PVA	1	30	1.5:0.5	2:50	60
F10	GMS	PLX 188	2	10	1:1	2:25	60
F11	GMS	PLX 188	1	30	1:1	2:50	60
F12	GMS	PLX 188	1	10	1.5:0.5	2:25	120

CHOL; Cholesterol, GMS; Glycerin monostearate, PVA; Polyvinyl alcohol, PLX; Poloxamer.

Table 2. Designed formulations, variables, and levels for further evaluation of budesonide nanoparticles using Box-Behnken method (lipid type, glycerin monostearate; surfactant type, polyvinyl alcoho; volume ratio of acetone/ethanol, 1.5:0.5; volume ratio of organic phase/aqueous phase, 2:50).

Formulations	PVA concentration (%)	GMS/drug	Sonication time (s)
F1	1.0	20	60
F2	1.5	20	30
F3	1.0	30	30
F4	0.5	20	30
F5	0.5	10	60
F6	1.0	30	90
F7	1.0	10	90
F8	0.5	20	90
F9	1.0	20	60
F10	1.5	20	90
F11	1.5	30	60
F12	1.0	20	60
F13	0.5	30	60
F14	1.0	10	30
F15	1.5	10	60
F16	1.0	20	60
F17	1.0	20	60

Bud; Budesonide, GMS; Gycerin monostearate, PVA; Polyvinyl alcohol.

Entrapment efficiency and loading percent determination

Entrapment efficiency was determined by measuring the concentration of unentrapped free drug in aqueous medium containing either PVA or PLX. About 1 ml of the Bud-SLNs dispersion was placed in the Ependorf tubes and centrifuged at 17000 rpm for 30 min. The nanoparticles along with encapsulated drug were separated at the bottom of the tubes. Plain SLN without budesonide was used as blank sample and centrifuged in the same manner.

In order to measure the free drug concentration, the UV absorbance of the supernatant was determined at 248 nm.

To eliminate the possible effects of free polymers upon the acquired absorbance, the blank sample undergoing the same procedure was subjected to the same process of spectrophotometric evaluation. The resulting absorbance was then subtracted from that of the samples, which present the net absorbance related to the free drug available within the supernatant.

This acquired absorbance was then used to calculate the free budesonide concentration based on the previously constructed calibration curve. Total amount of free drug was calculated and subtracted from the total utilized drug weight, yielding the weight of budesonide trapped in the particles.

The EE% and LP were calculated using the following equations:

$$EE\ (\%) = \frac{a \times 100}{b} \quad (1)$$

where, a is the weight of the drug in the nanoparticles and b is the weight of the drug used in the formulation

$$LP\ (\%) = \frac{c \times 100}{d} \quad (2)$$

where, c is the weight of the drug in the nanoparticles and d is the weight of the SLN.

Particle size and zeta potential analyses

PS and ZP were measured by photon correlation spectroscopy using Zetasizer Nano ZS (Malvern Instruments Ltd, UK). All measurements were carried out at 25 °C and performed in triplicate.

Scanning electron microscopy observation

Scanning electron micrographs were performed using an AIS-2100 scanning electron microscope (SEM, AIS-2100 SERON TECHNOLOGY, South Korea). A drop of the optimized SLN dispersion was mounted on aluminium stubs covered with a glass lamella, air dried, gold coated under vacuum, and then examined.

In vitro drug release study

To determine the release rate of budesonide from nanoparticles, 5 ml of aqueous dispersion of each formulation was transferred to the dialysis tubes with a molecular weight cutoff of 12000 Da and the sealed tubes were placed in the glass beaker in 40 ml of the phosphate buffered saline (PBS) 0.1 M, pH 7.4, 37 ± 0.5 °C with agitation at 150 rpm. Samples were withdrawn at predetermined time intervals and replaced with fresh PBS maintained at the same temperature. The content of budesonide in the samples was determined at 248 nm (24).Based on the plotted release profiles, MRT was calculated using following equation

$$MDT = \frac{\sum_{i=1}^{n} t_{mid} \times \Delta M_i}{\sum_{i=1}^{n} \Delta M_i} \quad (3)$$

where, *i* is the sampling number, *n* the number of dissolution sample time, t_{mid} the time at midpoint between t_i and t_{i-1} [easily calculated with the expression $(t_i+t_{i-1})/2$] and ΔM_i is the additional amount of drug dissolved between t_i and t_{i-1} (25).

In order to evaluate the drug release kinetics and mechanism, the release profiles were fitted into zero-order kinetics, first-order kinetics, Higuchi model, Hixon-crowell model, and Peppas equation, as indicated in Table 3.

Spray drying

Budesonide-loaded SLNs were prepared as described previously, and the optimized formulation was selected for spray drying to produce respirable microparticles. Lactose and mannitol were used as sugar carriers for the spray-drying process.

Optimized formulation (1 part) was mixed with lactose or mannitol (3 parts) for 15 min. Mixtures were spray dried using a Buchi B-191 mini spray dryer (BUCHI Labortechnik AG, Flawil, Switzerland) at an inlet temperature of 80 ºC, outlet temperature of 75 ºC, aspiration setting of 85% and spray flow of 400 NI/h. Immediately after the termination of the process, spray-dried lactose/mannitol particles were packed into tightly closed amber bottles.

The shape and surface morphology of the particles were studied by an SEM. A Next Generation Pharmaceutical Impactor (NGI, Apparatus E; British Pharmacopoeia, 2010) (Copley Scientific, Nottingham, UK) was used to determine the aerodynamic properties of the Bud-SLN co-spray dried with lactose or mannitol.

Table 3. Mathematical functions describing release rate of budesonide.

Function	Equation
Zero order kinetics	$W_R = K_0\ t \pm b$
First order kinetics	$\ln (W_L) = \ln W_0 - K_1 t$
Higuchi model	$W_R = K_H t^{1/2}$
Hixon-crowell model	$(W_L)^{1/3} = (W_0)^{1/3} - K_{HC} t$
Drug diffusion mechanism (Peppas equation)	$\text{Log}\ (M_t/M_\infty) = \log k + n\ \text{lot}$

Where, W_R is the amount of drug released at the sampling time t, W_L is the amount of drug remained within the dosage form at the sampling time t, W_0 is the initial amount of drug within the formulation, and K is the drug release rate constant, M_T is the amount of drug released up to the time t, M is the total amount of drug released up to time t.

The powders were filled into size 3 capsules and aerosolized using a Aerolizer®, a commercially available, breath-actuated, single dose capsule-based DPI. The DPI was attached to the induction port of the NGI by a molded silicone adapter and actuated over 4 s at a flow rate of 60 L/min. After aerosolization, all collection surfaces were rinsed with deionized water to dissolve carriers (lactose or mannitol) and then decanted with known volumes of chloroform for drug extraction from the nanoparticles. Then drug content in each stage was determined by UV spectrophotometer at 260 nm.

Mass median aerodynamic diameter (MMAD) and geometric standard deviation (GSD) were calculated with CITDAS V3.10, a data processing software (Copley Scientific.) based on the dose deposited on stages 1 through 7 and the micro-orifice collector (MOC), as defined in the USP 32-NF 27 General Chapter 601:

Aerosols, Nasal sprays, Metered-dose inhalers, and Dry powder inhalers. Fine particle fraction (FPF) was determined from the amount of budesonide collected from stages 2 through MOC, which represents the percentage of emitted particles with an MMAD of 4.5 μm or less. FPF estimates the fraction of particles expected to deposit deep within the lungs.

RESULTS

Taguchi design analyses

Several process parameters including lipid type, surfactant type, surfactant concentration (%), weight ratio of lipid to drug, volume ratio of acetone to ethanol, volume ratio of organic phase to aqueous phase, and sonication time were assessed. A number of nanoparticle formulations (Table 1) were prepared and the basic characteristics of the products were determined. Table 4 shows the results of PS, ZP, EE, LP and MRT of the studied formulations. Percent contribution of each variable on the different responses is also illustrated in Fig 1.

Table 4. Taguchi design along with the obtained responses.

Formulations	Dependent variables (responses)				
	PS (nm)	ZP (mV)	EE (%)	LP (%)	MRT (h)
F1	155.7 ± 3.8	-10.0 ± 0.82	87.2 ± 1.9	8.0 ± 0.18	7.9 ± 0.22
F2	225.9 ± 6.3	-13.1 ± 0.79	89.5 ± 2.8	8.2 ± 0.27	7.7 ± 0.25
F3	221.2 ± 4.1	-15.3 ± 0.98	87.7 ± 1.3	2.8 ± 0.31	6.5 ± 0.23
F4	204.6 ± 4.9	-12.7 ± 0.82	80.7 ± 1.7	2.5 ± 0.08	6.4 ± 0.20
F5	166.1 ± 3.8	-12.6 ± 0.57	77.6 ± 1.2	7.4 ± 0.19	5.8 ± 0.22
F6	151.1 ± 4.6	-15.6 ± 0.78	78.3 ± 1.4	2.5 ± 0.06	4.3 ± 0.20
F7	241.0 ± 7.2	-24.4 ± 1.58	82.6 ± 1.6	2.6 ± 0.11	9.7 ± 0.35
F8	194.7 ± 1.8	-21.9 ± 0.82	80.6 ± 1.7	8.5 ± 0.19	10.4 ± 0.19
F9	181.2 ± 3.5	-23.3 ± 1.66	93.6 ± 3.5	2.6 ± 0.97	11.6 ± 0.25
F10	143.0 ± 2.1	-12.1 ± 0.67	71.5 ± 1.6	6.6 ± 0.14	4.2 ± 0.16
F11	138.1 ± 5.5	-14.1 ± 0.45	78.7 ± 1.5	2.5 ± 0.08	5.5 ± 0.42
F12	165.5 ± 4.8	-17.1 ± 0.72	85.0 ± 1.3	7.8 ± 0.09	4.5 ± 0.29

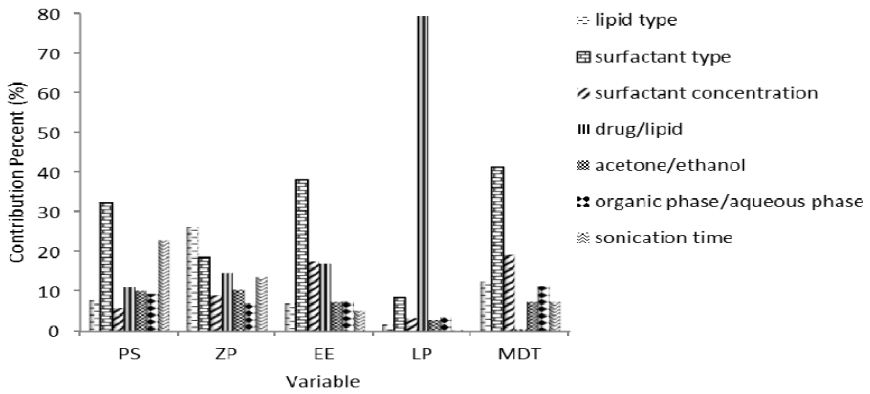

Fig. 1. Contribution percent of variables on responses in Taguchi design.

Box-Behnken design analyses

Based on the results from the analyses of the responses obtained from Taguchi design, three different independent variables including surfactant concentration (%), lipid to drug ratio (w/w), and sonication time (s) were selected for further investigation using Box-Behnken design. A number of nanoparticle formulations as given in Table 2 were manufactured and their basic characteristics were determined. Table 5 demonstrates the obtained responses measured for each formulation selected by the Box-Behnken design. The best fit models generated by the software (Design Expert 7®) for the observed responses included a 2FI model for PS (Y_1), a quadratic model for ZP (Y_2), a 2FI model for EE (Y_3), a 2FI model for LP (Y_4), and a quadratic model for MRT (Y_5). A summary of the statistical analyses for the response is shown in Table 6.

The effect of each factor on the obtained responses is shown in each equation and the P values indicating the significance of the differences each variable causes are given. The coefficient of each variable shows the contributing effect of that factor on the obtained response and the plus or minus sign signifies its boosting or castrating impact.

Table 5. Box-Behnken design along with the obtained responses.

Formulations	Dependent variables (responses)				
	PS (nm)	ZP (MV)	EE (%)	LP (%)	MRT (h)
F1	214.3 ± 5.1	-29.1 ± 1.9	91.9 ± 2.4	5.7 ± 0.32	9.4 ± 0.47
F2	173.7 ± 4.7	-27.6 ± 1.6	82.1 ± 1.5	5.1 ± 0.12	11.7 ± 0.62
F3	227.9 ± 8.1	-27.8 ± 1.1	93.6 ± 2.9	3.2 ± 0.11	10.5 ± 0.51
F4	239.3 ± 6.4	-21.7 ± 0.7	95.7 ± 2.2	5.9 ± 0.15	11.7 ± 0.47
F5	233.3 ± 5.1	-20.1 ± 0.9	94.4 ± 2.6	8.5 ± 0.25	10.9 ± 0.63
F6	238.7 ± 4.7	-29.4 ± 1.6	94.2 ± 3.4	3.4 ± 0.14	11.5 ± 0.92
F7	229.9 ± 2.0	-26.9 ± 1.7	89.2 ± 1.7	8.1 ± 0.21	10.3 ± 0.53
F8	247.9 ± 6.3	-20.8 ± 1.1	95.1 ± 1.0	5.5 ± 0.07	11.6 ± 0.74
F9	209.7 ± 5.8	-30.1 ± 1.6	87.1 ± 1.9	5.5 ± 0.17	8.8 ± 0.45
F10	182.7 ± 6.2	-27.2 ± 0.9	82.2 ± 1.6	5.4 ± 0.12	11.9 ± 0.32
F11	190.3 ± 3.2	-26.5 ± 1.3	82.2 ± 1.8	2.5 ± 0.06	12.3 ± 0.57
F12	194.1 ± 4.3	-31.8 ± 1.8	82.6 ± 1.3	5.7 ± 0.12	8.3 ± 0.24
F13	251.7 ± 7.2	-19.9 ± 1.9	95.5 ± 2.5	3.8 ± 0.09	11.8 ± 0.73
F14	206.7 ± 2.0	-27.3 ± 1.2	84.7 ± 1.5	7.7 ± 0.15	8.1 ± 0.65
F15	159.1 ± 6.9	-26.7 ± 1.7	81.4 ± 0.4	7.4 ± 0.08	11.6 ± 0.9
F16	216.7 ± 5.5	-29.9 ± 2.8	92.5 ± 2.5	5.7 ± 0.17	9.8 ± 0.48
F17	199.6 ± 4.4	-28.6 ± 2.4	84.8 ± 0.8	5.3 ± 0.11	8.8 ± 0.37

PS; Particle size, ZP; Zeta potential, EE; Eentrapment efficiency, LP; Loading percent, MDT; Mmean dissolution time.

Table 6. Summary of the statistical analyses of the responses generated by Box-Behnken.

Source	PS (Y_1)		ZP (Y_2)		EE (Y_3)		LP (Y_4)		MDT (Y_5)	
	Coeff.	P value	Coeff.	P value	Coeff.	P value	Coeff.	P value	Coeff.	P value
		0.0005 (sig.)		0.0004 (sig.)		0.0087 (sig.)		0.0001 (sig.)		0.0077 (sig.)
Intercept	212	-	29.9	-	88.7	-	5.48	-	9.07	-
X_1	-33.3	0.0001	3.19	0.0001	-6.50	0.0003	-0.4	0.0001	0.22	0.3673
X_2	9.95	0.0390	0.34	0.4007	1.97	0.1273	-2.5	0.0001	0.61	0.0291
X_3	6.43	0.1560	-0.22	0.9549	0.66	0.5892	0.055	0.4361	0.48	0.0675
X_1X_2	3.21	0.6000	-5.000	0.9929	-0.050	0.9767	0.19	0.0757	-0.12	0.7221
X_1X_3	0.19	0.9757	0.12	0.8281	-5.000	0.9977	-2.5	0.9799	-0.08	0.8082
X_2X_3	-3.10	0.6121	0.51	0.3814	-0.96	0.5769	-0.097	0.3332	-0.31	0.3685
X_1^2	-	-	-5.07	0.0001	-	-	-	-	2.02	0.0003
X_2^2	-	-	-1.51	0.0246	-	-	-	-	0.51	0.1410
X_3^2	-	-	-0.50	0.3743	-	-	-	-	0.55	0.1182
Lack of fit	-	0.2889 (non sig.)	-	0.7065 (non sig.)	-	0.8875 (non sig.)	-	0.9643 (non sig.)	-	0.3751 (non sig.)

Particle size

Based on the analyses using Design Expert 7®, and the related modeling, the following equation was obtained which shows the effect of each factor on the resulted PS (equation 4):

$$Y_1 = 212.68 - 33.32X_1 + 9.95X_2 + 6.43X_3 + 3.21\ X_1X_2 + 0.19X_1X_3 - 3.1X_2X_3 \quad (4)$$

where, Y_1 is the PS, and X_1, X_2, and X_3 are surfactant concentration, weight ratio of lipid/drug and sonication time, respectively. Fig. 2 shows the 3D surface response plots for the PS analyses.

Zeta potential

The ZPs measured for all formulations were negative. For the analyses of the obtained data, however, ZP was considered in its absolute value, and with no minus or plus sign. The results obtained for the ZP of the prepared nanoparticles are listed in Table 5. Equation 5 demonstrates the effect of each factor on the obtained ZP. Corresponding P values are reported in Table 6.

$$Y_2 = 29.93 + 3.19X_1 + 0.34X_2 \quad -0.022X_3 - 5.07X_1^2 - 1.51X_2^2 - 0.5X_3^2 - 5.000$$

$$E\text{-}003X_1X_2 + 0.12X_1X_3 + 0.51X_2X \quad (5)$$

where, Y_2 is the ZP, and X_1, X_2, and X_3 are as defined already. Fig. 3 depicts the 3D surface response plots for ZP analyses.

Entrapment efficiency and loading percent

The EE% and LP for each formulation selected by Box-Behnken design is tabulated in Table 5. The effect of each factor on the obtained EE% is demonstrated in equation 6 and on LP is shown in equation 7. Respective P values are also given in Table 6.

$$Y_3 = 88.78 - 6.5X_1 + 1.97X_2 + 0.66X_3 - 0.05X_1X_2 - 5.000E\text{-}003X_1X_3 - 0.96X_2X_3 \quad (6)$$

$$Y_4 = 5.48 - 0.4X_1 - 2.5X_2 + 0.055X_3 + 0.19X_1X_2 - 2.500E\text{-}003X_1X_3 - 0.097X_2X_3 \quad (7)$$

where, Y_3 is the EE%, Y_4 is the LP, and X_1, X_2, and X_3 are as previously defined. Figures 4 and 5 demonstrate the 3D surface response for the EE% and LP analyses, repectively.

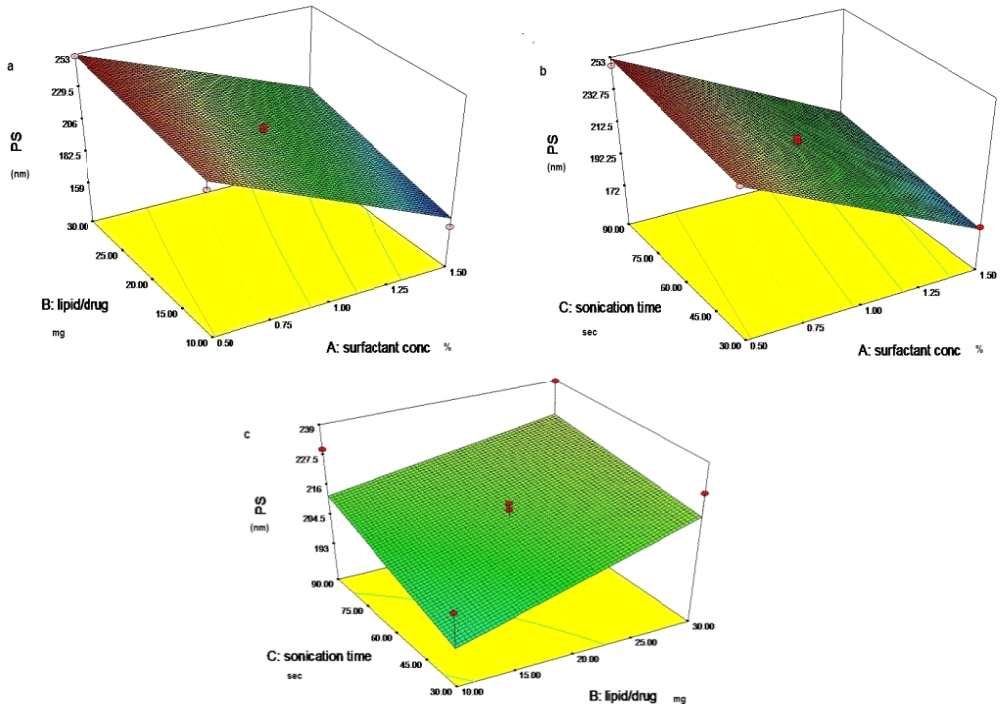

Fig. 2. 3D surface response plots for PS analyses: a) PS vs lipid/drug and surfactant concentration, b) PS vs sonication time and surfactant concentration, c) PS vs sonication time and lipid/drug

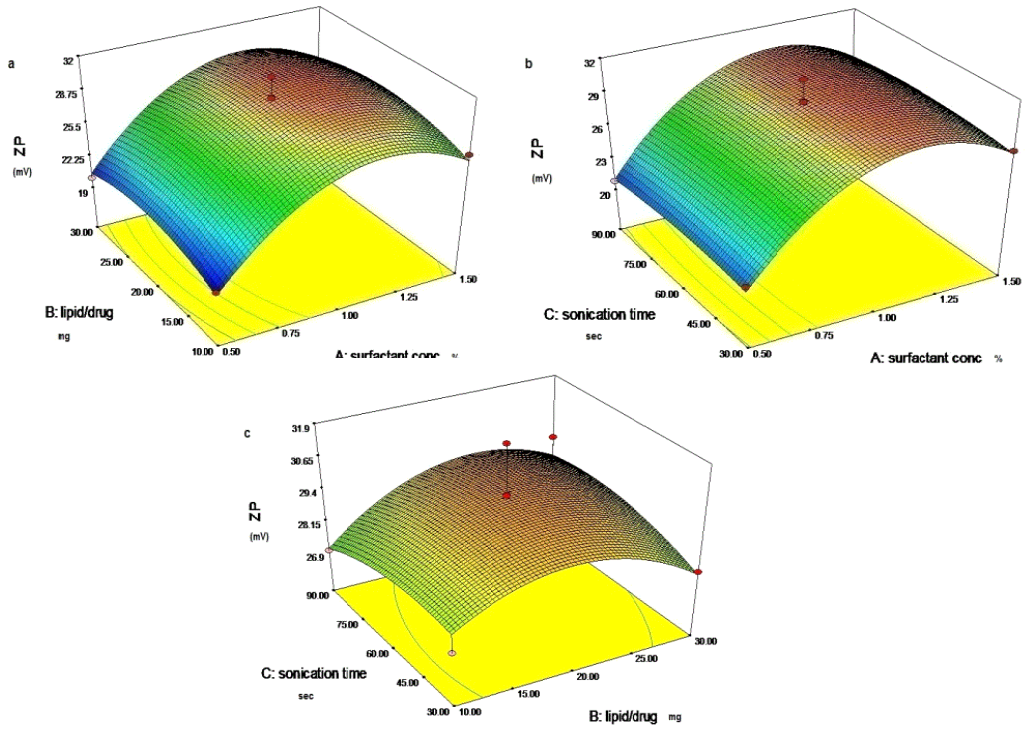

Fig. 3. 3D surface response plots for ZP analyses: a) ZP vs lipid/drug and surfactant concentration, b) ZP vs sonication time and surfactant concentration, c) ZP vs sonication time and lipid/drug.

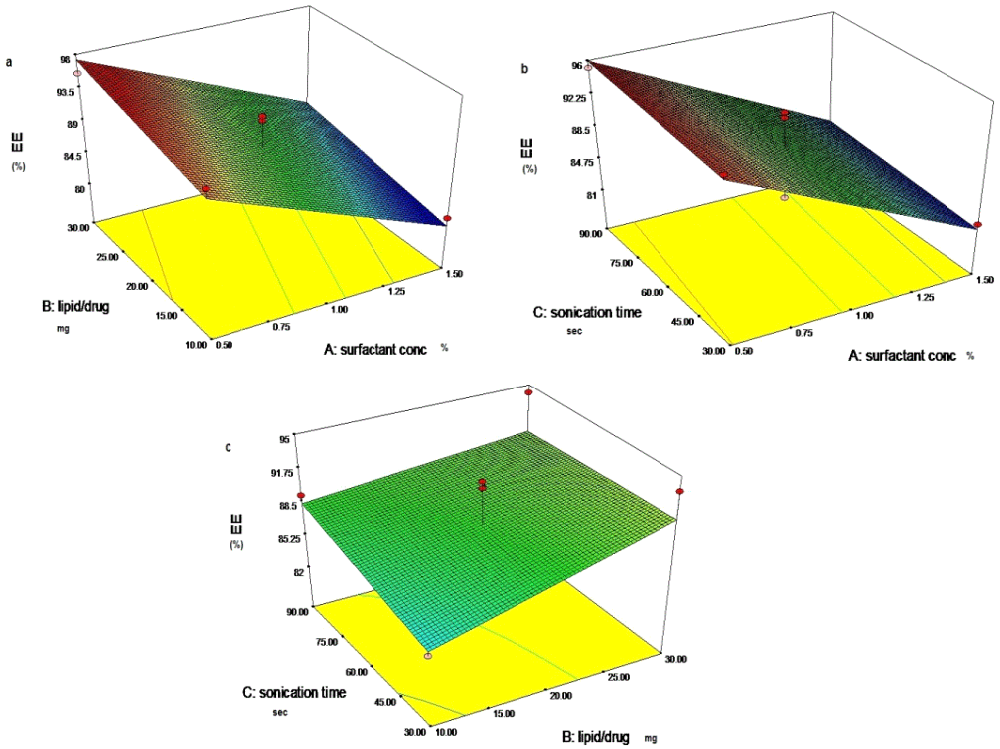

Fig. 4. 3D surface response plots for EE analyses: a) EE vs lipid/drug and surfactant concentration, b) EE vs sonication time and surfactant concentration, c) EE vs sonication time and lipid/drug.

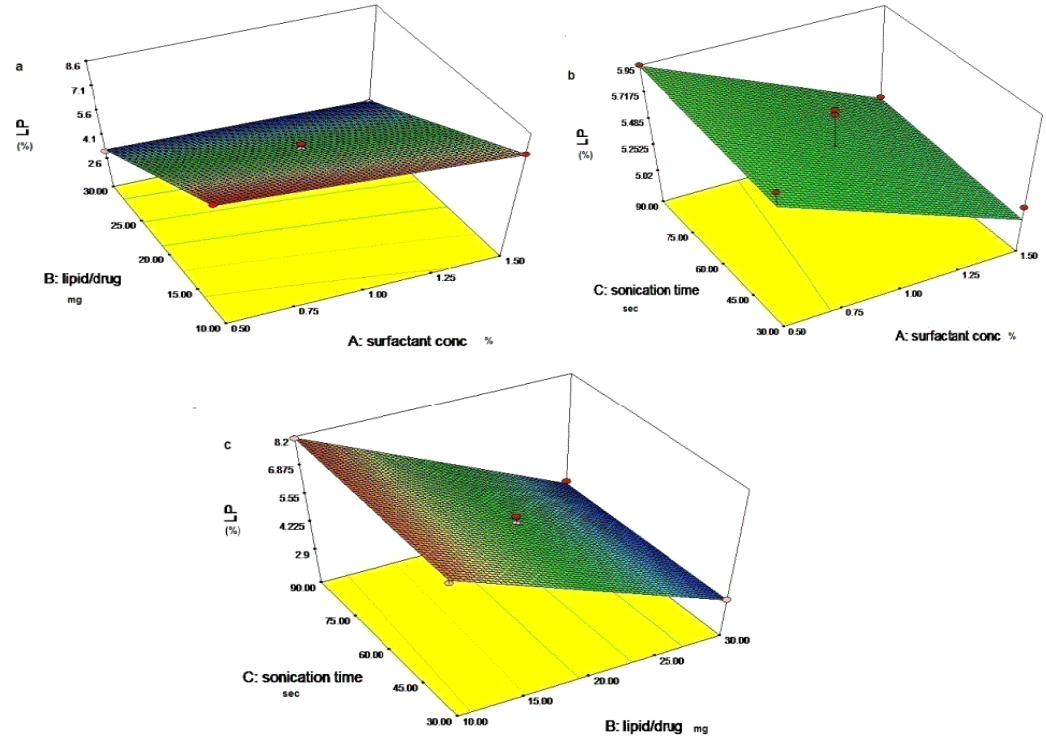

Fig. 5. 3D surface response plots for loading percent analyses: a) LP vs lipid/drug and surfactant concentration, b) LP vs sonication time and surfactant concentration, c) LP vs sonication time and lipid/drug.

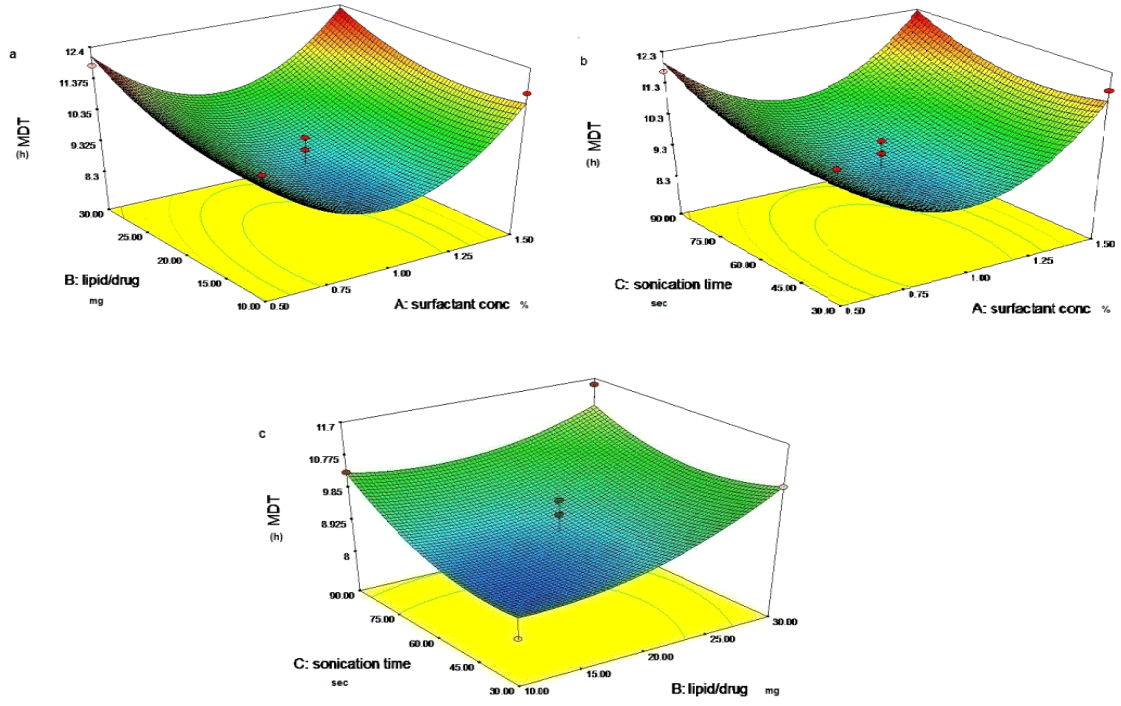

Fig 6. 3D surface response plots for MDT analyses: a) MDT vs lipid/drug and surfactant concentration, b) MDT vs sonication time and surfactant concentration, c) MDT vs sonication time and lipid/drug.

Release studies and mean release time

The calculated MRT values are presented in table 5. The effect of each factor on the obtained MDT is shown in equation 8 and the related P values which signify the effect of each variable are given in Table 6.

$$Y_5 = 9.07 + 0.22X_1 + 0.61X_2 + 0.48X_3 + 2.02X_1^2 + 0.51X_2^2 + 0.55X_3^2 - 0.12X_1X_2 - 0.08X_1X_3 - 0.31X_2X_3 \quad (8)$$

where, Y_5 is the MDT, and X_1, X_2, and X_3 are as already defined. Fig. 6 shows the 3D surface response plots for the MDT analyses.

Drug release kinetics and mechanism

Budesonide release kinetics from the prepared nanoparticles using Taguchi and Box-Behnken designs indicated that the release kinetics of the majority of the formulations conform to the either Zero- or first-order kinetics, while some of them can be fitted in the Higuchi or Hixon-Crowell models. The release mechanism was determined based on the values calculated for n through the Peppas equation.

In case of the diffusion mechanism, results suggested that the vast majority of the formulations conformed to the case II mechanism, while few followed Fickian diffusion mechanism (data are not shown).

Optimization

Based on the modeling by Design Expert 7®, the following values were suggested by the software to prepare the optimized formulation: 1.2% surfactant concentration, lipid-to-drug weight ratio of 10 and a sonication time of 90 s.

The optimized formulation was then prepared and all the necessary evaluations concerning the PS, ZP, LP, MDT, EE% and release kinetics and mechanism were made subsequently. Table 7 shows the average values for each result both predicted by the software and obtained through the experiment. The error percent for predicted and observed values is also reported.

Scanning electron microscope observation of optimized nanoparticles

The SEM image of optimized nanoparticle is shown in Fig. 7. The image clearly displays the size and the morphology of the optimal design. Scanning electron microscopy studies revealed that budesonide-loaded SLN were almost spherical in shape with a smooth morphology (Fig.7).

Drug release profile of optimized nanoparticles

The prepared optimized nanoparticle was evaluated in terms of the drug release kinetics and drug diffusion mechanism. As illustrated in Fig. 8, more than 95% of budesonide was released from the nanoparticles within 24 h. There was a very short lag time of about one h in early stage of the release profile which was then followed by a sustained manner for up to 24 h seen typically in the controlled release delivery systems. As it is evident from table 7, the release kinetics of the optimized formulation was best conformed to the Higuchi model. The n value for the release profile of this formulation was equal to 0.8.

Table 7. Predicted and acquired results for the optimal formulation along with the calculated error (%).

Responses	PS (nm)	ZP (mV)	EE (%)	LP (%)	MDT (h)	n value	K_R	R^2
Actual values	218.2 ± 6.6	-26.7 ± 1.9	92.5 ± 1.52	5.8 ± 0.25	10.4 ± 0.39			
Predicted values	200.9	-27.5	86.4	7.91	10.6			
Error (%)	8.82	3.08	7.11	-26.9	-1.42			
Zero order							0.075	0.917
First order							0.111	0.977
Higuchi model							0.453	0.986
Hixon-Crowell							0.031	0.976
Peppas equation						0.811		

Table 8. Aerodynamic properties of dry powder inhaler formulations of Bud-loaded nanoparticles.

Sample	Aerodynamic properties		
	FPF (%)	MMAD (µm)	GSD (µm)
Mannitol	33.75	2.33	3.07
Lactose	49.5	2.06	2.98

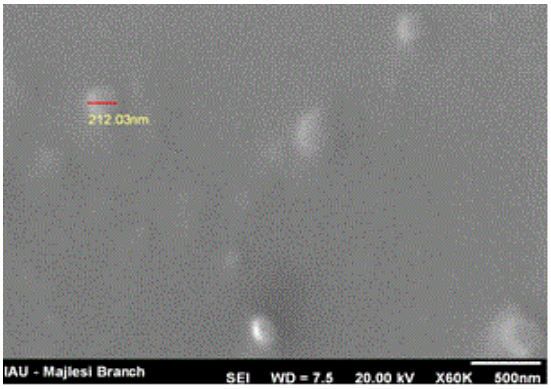

Fig. 7. Scanning electron microscopy imaging of the prepared nanoparticle

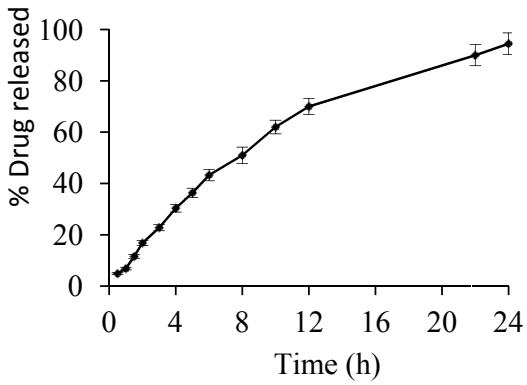

Fig. 8. Drug release profile from the optimized formulation

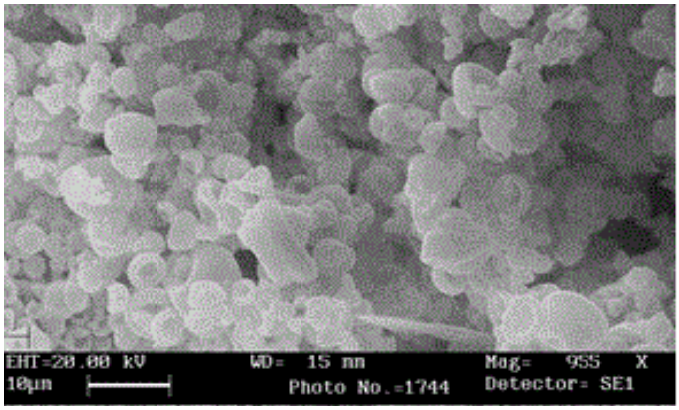

Fig. 9. Scanning electron microscopy photo of spray dried optimized formulation with lactose at ratio of 1:3.

Spray drying

The aerodynamic properties of the budesonide-loaded nanoparticles co-spray dried with lactose or mannitol are shown in Table 8. Comparing two formulations, one prepared from optimized formulation and lactose at a ratio of 1:3 displayed better aerodynamic properties from the Aerolizer® DPI. This formulation showed the highest fine particle fraction (FPF) and the lowest geometric standard deviation (GSD) and MMAD.

SEM image of spray-dried of optimized formulation with lactose at a ratio of 1:3 is shown in Fig. 9.

DISCUSSION

The Box-Behnken design is a relatively complicated design facilitating a more in-depth interpretation of the data, though it requires a much higher number of experiments to be conducted. Therefore, for each additional variable, a remarkable number of experiments will be added to the design matrix. Since we intended to investigate the impact of seven different variables on the responses, the design matrix would be immense indeed. Therefore, it was necessary to rule out the insignificant variables beforehand, in order to avoid this large design matrix. This was fulfilled using the Taguchi design which, due to the assessment of the variables in extreme levels, provides a considerably more limited number of the experiments, and can thus conveniently serve the aforementioned purpose.

Taguchi design analyses

PS is one the most important characteristics of the nanoparticles, affecting both the release pattern of the drug and its absorption (26). Statistical analyses revealed that the most effective factor on the PS relates to the effect of the surfactant type and lipid/drug ratio (Fig. 1). With the increase of lipid content, the mean PS of SLNs increased (Table 4). The fact that

the size of lipid nanoparticles is highly dependent on lipid concentration can be explained in terms of the tendency of the lipid to coalesce at high lipid concentration. According to Stokes' law, this behavior can be explained by a difference in density between the internal and external phases (27). For instance, Patel and coworkers reported that an increase in GMS concentration led to the formation of flakes (28). Another group of scientists, Sarmento and colleagues, also found that PS tends to increase following the increment of lipid/surfactant mass ratio, while the reduction of the ratio led to the production of particles of smaller sizes (29). In another study, Arora and coworkers found that an increase in lipid concentration leads to the formation of particles of bigger sizes (30). As shown in Fig.1 and Table 4 the sonication time and acetone/ethanol volume ratio also contribute to the PS. Increasing the sonication time and acetone/ethanol volume ratio from level 1 to level 2 both increased the PS of the nanoparticles but not considerably. By increasing the sonication time, PS was moderately increased. Because of turbulent flow and shocking waves generated by cavitation in liquids irradiated with ultrasound, particles are associated together at extremely high speeds inducing effective melting at the point of impact and contribute to the facile agglomeration process (31). It was found in the present investigation that an increase in the sonication time led to the increase in PS. The finding is in accordance with other investigations such as those conducted by Zengshuan and colleagues l who reported that slower sonication time corresponds to smaller PS values (32) and Motwani and coworkers who reported a significant increase of the PS following the increment of sonication time from 60 to 240 s (33). Bouchemal and colleagues have shown that the nanoemulsions obtained using acetone or ethanol presented homogeneous particles without aggregates or phase separation (34). Acetone is miscible with water and is the most appropriate solvent; however, the high inflammability limits its industrial use. For this reason, the effect of acetone substitution with ethanol in different ratios of acetone/ethanol 1:1 and 3:1 was studied. The results showed that with increasing acetone fraction, the particle size increased though not significant. Bouchemal and coworkers showed that incorporation of acetone with a low water-miscible solvent caused a better size distribution and smaller PS with increase in acetone ratio (37), while in our study both acetone and ethanol are water-miscible solvents. Another study showed the use of acetone as an organic solvent caused significantly larger nanoparticles with a Z-average of more than 200 nm and a PI of around 0.21 with respect to ethanol (35). Increasing the concentration of surfactant increased the PS of the nanoparticles (Table 4 and Fig. 1). Muller (36) has shown that increasing the PLX concentration to 1% was effective in producing smaller size SLN in case of tripalmitin, cetyl palmitate and GMS. It was concluded that further increase in PLX concentration to 1.5% did not reduce the PS. These results clearly suggested that 1% of surfactant was sufficient to cover the surface of nanoparticles effectively and prevented agglomeration during the homogenization process. They avoided the high concentration of surfactant (1.5%) to prevent decrease in the EE and also the toxic effects associated with surfactants (37).

Analysis of ZP data (Table 4 and Fig. 1) revealed that the type of the lipid is the most effective ($p<0.05$) variable on ZP of the nanoparticles. ZP was increased by changing lipid from cholesterol to GMS. Surfactant type and the lipid to drug content had also significantly contributed to the ZP. While alteration of surfactant from PVA to PLX decreased the ZP, increasing the lipid to drug content from level 1 to level 2 increased the extent of this parameter. Though not significant, absolute ZP of the particles increased as the emulsifier concentration increased from 1 to 2%.

ZP is the measure of overall charges acquired by particles in a particular medium and is considered as one of the benchmarks of the stability of colloidal systems. Particles will repel each other if the systems have high positive or negative value of ZP. A system having value of ± 30 mv is considered a stable formulation if dispersed in a liquid as colloidal

dispersion (38). The incorporation of drug showed little effect on the ZP (39). Muller and coworkers (40) have reported that potentials between -5 and -15 mV are in the region of limited flocculation; and between -5 and -3 mV are in the region of maximum flocculation (41). In cases where a sterically stabilizing surfactant presents in the surfactant mixture, even lower ZP are sufficient for a stable suspension.

The negative charge of SLN may result from fatty acids released from the hydrolysis of GMS. In such a system, the hydrophilic emulsifiers were thought to align alongside each other, imparting more rigidity and strength to the emulsifier film through hydrogen bonding. Changing the lipid type from GMS to CHOL decreased the absolute value of zeta potential. Actually crystalline re-orientation of lipid can result in alteration of the charges on the particle surface and subsequently the measured ZP (42).

Poloxamer 188 as a non-ionic surfactant tends to reduce the absolute value of ZP (43). ZP is also a function of surface coverage by charged species at a specified pH. Despite the fact that PVA is classified as a nonionic polymer, its macromolecules contain besides hydroxyl groups some acetate ones. These groups come from uncompleted hydrolysis of polyvinyl acetate in the production process of PVA. Thus, its macromolecules contain acetate groups. The C—H bonds in α position in relation to acetate groups have acidic properties. In this way the acetate groups in PVA macromolecules gain negative charge which results in more negative ZPs (44).

In our study, the contribution of lipid on ZP was more than other factors which may be because of the high concentration of lipid in the emulsion.

High surfactant concentrations effectively stabilize the particle created by forming a steric barrier on the particle surface, thereby protecting the particles from coagulation (45). As mentioned earlier, the acetate groups in PVA macromolecules gain negative charge and at higher concentrations results in more negative ZPs.

The EE and LP as well as the impact of each factor on these parameters for each formulation are given in Table 4 and Fig. 1. It was observed that surfactant type as well as surfactant concentration significantly affected the EE%. With respect to the EE%, change of surfactant from PVA to PLX and increasing surfactant concentration from l% to 2% led to a lower EE%. Changing the lipid/drug weight ratio from level 1 to 2 increased the drug loading that relates to good entrapment of drug in the lipids. Lipid type and other factors were not effective on drug loading.

The amount of drug to be incorporated into the delivery system is dependent on the physicochemical properties of drug and the preparation process. Overall, high EE was the result of high solubility of the drug in the melted lipid (46). The EE was decreased by increasing the amount of surfactant. This could be attributed to the increase in the solubility of budesonide in the aqueous phase as the percentage of surfactant increased, due to the solubilization effect of the emulsifier. Also part of the budesonide was incorporated in the surfactant layer at the surface of the SLN, leading to lower EE.

The result showed that the EE increased as the amount of lipid increased. Increasing the lipid content increased the EE% because of the increased solubilizing agents for highly lipophilic drugs and provided more and more spare space to accommodate excessive drugs (47). This effect was probably also due to the increased viscosity of the medium, because increasing the amount of lipid resulted in faster solidification of the nanoparticles. This would also prevent drug diffusion to the external phase of the medium (48). Similar results are reported by Reddy and coworkers (49). While increasing the weight ratio of lipid to drug resulted in a significant increase in EE, LP value was considerably reduced. Since the amount of drug loaded within the particles undergoes little changes with the changes in processing variables, an increase in the content of the lipid led to the decrease of the overall fraction and the resulted LP. Other variables found to be of little importance (Table 4).

Fig. 1 shows that the drug release from SLNs is significantly affected by surfactant type. PVA resulted in much slower release (greater MRT) than PLX. All other variables

decreased the release rate moderately when increased from level 1 to level 2.

In fact, as the particle size decreases as it occurs with PLX compared to PVA, the available surface area increases and the release rate is increased consequently. The esterification of glycerol by long-chain fatty acids is responsible for high hydrophobicity of these glycerides. This may explain the slow release of the drug from SLNs containing GMS (50-53).

Lipid to drug weight ratio could influence the release of the budesonide from nanoparticles. When the lipid to drug content increased, the size of the particles was increased and consequently the specific surface area was decreased and slower release rate was observed (54). Increasing the amount of lipid resulted in increased viscosity of the medium and more rigid solidified nanoparticles. This would also retard the drug diffusion to the dissolution medium.

Increasing the sonication time decreased the drug release percentage that may be because of more interaction between particles, more aggregation and increasing the size as well as decreasing its surface area. Similar sustained-release of clozapine was observed from tripalmitin-SLN prepared by the homogenization followed by ultrasonication method (55). Kumara and colleagues (56) reported that cetyl palmitate SLNs also demonstrated controlled-release profiles. In addition, in the current study in most tested SLN formulations, an almost rapid release was observed in the first 6 h that reached about 50% of the overall budesonide released from each formulation. This could be due to the drug-enriched shell around the particles. Slow diffusion of the lipophilic drug from the lipid matrix prolonged the drug release from the nanoparticle formulations (57-58).

Box-Behnken design analyses

A simple review of Equation 4 generated by Design Expert 7® and the related P values (Table 6) demonstrates that surfactant concentration can affect the PS most significantly, while lipid to drug weight ratio is the second significantly effective factor. A linear correlation also exists between the surfactant concentration and the PS, i.e. the higher the surfactant concentration, the smaller the PS (Fig. 2a). The least effective factor is, of course, the sonication time. The present investigation found that an increase in the sonication time led to the increase of the PS (Fig. 2b and 2c). The finding is in accordance with other investigations, such as those conducted by Zengshuan and coworker who reported that longer sonication time corresponds with bigger PSs (32). At lower extremes of lipid to drug and sonication time smallest particles are produced (Fig. 2c). The particle size of the optimized formulation was found to be 218 nm which is desirable for pulmonary delivery of this drug .These findings are in accordance with the results obtained from Taguchi design and same discussions thus are applied.

Further analyses and statistical modeling (Table 6) revealed that, as predicted, surfactant concentration is the most important factor significantly affecting the ZP. Fig. 3 clearly demonstrates that greater ZP values are observed while high extreme concentrations of PVA are used. The stability of many colloidal systems is directly related to the magnitude of their ZP. The surface charge of the particles is of substantial importance in all the production steps of these particles, as the efficiency of the different steps is directly related to the establishment of electrostatic interactions (37). A ZP around ± 25 mV can be an indicator of assuring the stability of the particulate systems. The ZP of optimized formulation (-26.7) is good enough to stabilize the formulation.

A simple review of the attained EE for different formulations (Table 5) reveals that as the level of surfactant concentration increases, EE will decrease (Fig. 4a and 4b). This observation is in agreement with that found earlier and discussed in previous section. Highest EE is attained when higher extremes of sonication time and lipid to drug ratio are used (Fig. 4c).

On analyzing the response surfaces for LP, it was obvious that the level of lipid to drug ratio and surfactant exert influence on LP. When the amount of surfactant increased, the LP, though very small about 1%, was found to

decrease (Fig. 5b). At the same time, for constant amount of surfactant, when lipid/drug weight increased, the amount of excipients increased which resulted in reduced LP.

The MRT varied from 8.3 to 11.7 h for various factor levels (Table 5). The independent factor affecting the MRT was the lipid to drug ratio (Table 6). As the lipid content or sonication time increased, the MRT was increased (Fig. 6). The sonication time, to some extent, was also effective on MRT but its impact did not reach to a significant level (Table 6, P=0.06). Surfactant concentration did not exert any significant impact on MRT. It can be concluded from Fig. 6a and Fig. 6b that the particles sustained the release of the drug best when extreme values of both factors are combined. These observations are in the same directions of what observed in Taguchi design and same interpretations are applied.

The optimized formulation was evaluated for drug release kinetics and drug diffusion mechanism. The release kinetics of the optimized formulation was best fitted to the Higuchi model suggesting that drug release occurs as a diffusion controlled process based on the Fick's Law where the diffusion coefficient depends upon both the concentration and the time. Since n value for the release profile of this formulation was equal to 0.8, the release mechanism is assumed to follow case II mechanism where both erosion of the lipid and diffusion of the drug might be involved (59,60).

The optimized formulation co-spray dried with lactose (hybrid microparticles) displayed desirable FPF, MMAD, GSD of 49.5%, 2.06, and 2.98; respectively. Hybrid microparticles with FPF% as high as 40% has been previously reported (61).

Importantly, the microparticles have been shown to disassociate into the primary nanoparticles once they are exposed to an aqueous environment such as alveolar lung region. Therefore, the nanoparticles can remain in the lung lining fluid until absorption while avoiding unwanted phagocytic mechanism. More importantly, the physicochemical properties of nanoparticles and the release profile of the therapeutic agents are shown not to be affected by the spray-drying process (62,63).

CONCLUSION

This study has demonstrated the potential use of SLNs for the controlled release of budesonide used in the treatment of asthma. The Bud-SLNs prepared by the emulsification–solvent diffusion method exhibited high EE, particles of a suitable size range, and controlled release profile. Based on the optimization established by Design Expert 7® software, a formulation constituted of GMS, 1.2 % PVA, lipid to drug of 10 and 90 s sonication time was selected.

The mean PS, ZP, EE, LP, and MRT of adopted formulation was predicted and confirmed to be 218.2 nm (desirable for pulmonary delivery), -26.7 mV (good enough to stabilize the formulation), 92.5%, 5.83%, and 10.4 h, respectively. The release characteristics of adopted formulation indicate that the drug content could be released within a day which is desirable for pulmonary delivery of budesonide. The optimized formulation co-spray dried with lactose (hybrid microparticles) displayed desirable FPF, MMAD, and GSD of 49.5%, 2.06 μm, and 2.98 μm, respectively. Our results provide fundamental data for the application of SLNs in pulmonary delivery system of budesonide. Future studies should be conducted to evaluate the effectiveness of this system in vivo.

ACKNOWLEDGMENTS

The content of this paper is extracted from the Pharm.D thesis NO. 389235 submitted by H. Mohiti which was financially supported by the Research Department of Isfahan University of Medical Sciences, Isfahan, I.R. Iran.

REFERENCES

1. Geller D. Comparing clinical features of the nebulizer, metered dose inhaler, and dry powder inhaler. Respir Care. 2005;50:1313-1321.
2. Rau J. The inhalation of drugs: advantages and problems. Respir Care. 2005;50:367-382.
3. Pauwels R, Lofdahl C, Postma D. Effect of inhaled formoterol and budesonide on exacerbations of asthma. N Engl J Med. 1997;337:1405-1411.
4. Traini D, Young PM. Delivery of antibiotics to the respiratory tract for pulmonary infection. Adv Drug Deliv Rev. 2007;11:712-756.

5. Scheuch G, Kohlhaeufl MJ, Brand P, Siekmeier R. Clinical perspectives on pulmonary systemic and macromolecular delivery. Adv Drug Deliv Rev. 2006;58:996-1008.
6. Telko M, Hickey A. Dry powder inhaler formulation. Respir Care. 2005;50:1209-1227.
7. Sung JC, Pulliam BL, Edwards DA. Nanoparticles for drug delivery to the lungs. Trends Biotechnol. 2007;25:563-570.
8. Niven RW. Recent advances in liposomal dry powder formulations: preparation and evaluation. Crit Rev Ther Drug Carr Syst. 1995;12:151-231.
9. Bosquillon C, Lombry C, Preat V, Vanbever R. Characterization and aerosol dispersion performance of spray-dried chemotherapeutic PEGylated phospholipid particles for dry powder inhalation delivery in lung cancer. J Control Release. 2001;70:329-339.
10. Manjunath K, Reddy J, Venkateswarlu V. Solid lipid nanoparticles as drug delivery systems. Methods Find Exp Clin Pharmacol. 2005;27:127-144.
11. MeriskoLiversidge E, Liversidge GG, Cooper ER. Drug nanoparticles: formulating poorly water-soluble compounds. Eur J Pharm Sci. 2003; 18:113-120.
12. Sun H, Zhang XH, Wang S, Tu YF, Zhao RS, Xie YJ. Construction and properties of structure and size controlled micro/nano-particles. Chin Pharm Sci. 2011;20:259-265.
13. Wissing SA, Kayser O, Müller RH, Solid lipid nanoparticles for parenteral drug delivery. Adv Drug Deliv Rev. 2004;56:1257–1272.
14. Joshi MD, Müller RH. Lipid nanoparticles for parenteral delivery of actives. Eur J Pharm Biopharm. 2009;71(2):161-172.
15. Rabinnow BE, Kayser O, Lemke A. The impact of nanobiotechnology on the development of new drug delivery systems. Nat Rev Drug Dis. 2004;3:785-796.
16. Richard NF, Lana B, Wakure BS. Development of chitosan capsule for colon specific delivery of budesonide. Adv Drug Deliv Rev. 2005;57:303-316.
17. Rabinow BE. Nanosuspensions in drug delivery. Nat Rev Drug Discov. 2004;3:785–796.
18. Kesisoglou F, Panmai S, Wu Y. Nanosizing oral formulation development and biopharmaceutical evaluation. Adv Drug Deliv Rev. 2007;59:631–644.
19. Muller RH, Mader K, Gohla S. Solid lipid nanoparticles (SLN) for controlled drug delivery-a review of the state of the art. Eur J Pharm Biopharm. 2000;50:161–177.
20. El-Gendy N, Gorman EM, Munson EJ, Berkland C. Budesonide nanoparticle agglomerates as dry powder aerosols with rapid dissolution. J Pharma Sci, 2009;98:2731-2746
21. Jacobs C and Müller RH. Production and characterization of a budesonide nanosuspension for pulmonary administration. Pharma Res, 2002;19:189-194.
22. Sahib MN, Darwis Y, Peh KK, Abdulameer SA, Tze Y, Tan F. Rehydrated sterically stabilized phospholipid nanomicelles of budesonide for nebulization: physicochemical characterization and in vitro, in vivo evaluations. Int J Nanomed. 2011;6:2351–2366
23. Cook RO, Pannu RK, Kellaway IW. Novel sustained release microspheres for pulmonary drug delivery. J Control Release. 2005;104:79–90.
24. Muhlen A, Mehrnet W. Drug release and release mechanism of prednisolone loaded solid lipid nanoparticles. Pharmazie. 1998;53:552-577.
25. Costa P, Lobo JMS. Modeling and comparison of dissolution profiles. Eur J Pharm Sci. 2001;13:123-133.
26. Gazori T, Khoshayand MR, Azizi E, Yazdizadeh P, Nomani A, Haririan I. Evaluation of alginate/chitosan nanoparticles as antisense delivery vector: Formulation, optimization and in vitro characterization. Carbohyd_Polym. 2009;77:599-606.
27. Leroux J, Allémann E, Doelker E, Gurny R. New approach for the preparation of nanoparticles by an emulsification-diffusion method. Eur J Pharm Biopharm. 1995;41:14-18.
28. Patel JK, Patel RP, Amin AF, Patel MM. Formulation and evaluation of mucoadhesive glipizide microspheres. AAPS Pharm Sci Tech. 2005;6:49-55.
29. Sarmento B, Ferreira D, Veiga F, Ribeiro A. Characterization of insulin loaded alginate nanoparticles produced by inotropic pre-gelation through DSC and FTIR studies. Carbohyd_Polym. 2006;66:1-7.
30. Arora S, Gupta S, Narang RK, Buthiraja RD. Amoxicillin loaded chitosan-alginate polyelectrolyte complex nanoparticles as mucopenetrating delivery system for H.Pylori. Sci Pharm. 2011;79:673-694.
31. Prozorov T, Prozorov R, Suslick KS. High velocity interparticle collisions driven by ultrasound. J Am Chem Soc. 2004;126:13890-13891.
32. Zengshuan MA, Yeoh HH, Lim LY. Formulation pH modulates of insulin with chitosan nanoparticles. J Pharm Sci. 2002;91:1396-1404.
33. Motwani SK, Chopra S, Taleganokar S, Kohli K, Ahmad FJ, Khar RK. Chitosan-sodium alginate nanoparticles as submicroscopic reservoirs for ocular delivery: Formulation, optimization and in vitro characterization. Eur J Pharm Biopharm. 2008;68:513-525.
34. Bouchemal K, Briancon S, Perrier E, Fessi H. Nano-emulsion formulation using spontaneous emulsification: Solvent, oil and surfactant optimization. Int J Pharm. 2004;280:241-251.
35. Schubert MA, Muller-Goymann CC. Solvent injection as a new approach for manufacturing lipid nanoparticles: evaluation of the method and process parameters. Eur J Pharm Biopharm. 2003;55:125-131.
36. Muller RH. Lipid nanoparticles: recent advances. Adv Drug Del Rev. 2007;59:375-376.
37. Nazar MR, Hafeezullah K, Shahzad N. Encapsulation and characterization of controlled release flurbiprofen loaded microspheres using beeswax as an encapsulating agent. J Mater Sci. 2010;21:1621-1630.

38. Rahman Z, Zidan A, Habib M, Khan M. Understanding the quality of protein loaded PLGA nanoparticles variability by Plackett-Burman design. Int J Pharm. 2010;389:186-194.
39. Saulnier P, Pech B, Proust JE, Benoit JP. Physicochemical stability of colloidal lipid particles. Biomaterials. 2003;24:4283-4300.
40. Muller RH, Maeder K, Gohla S. Solid lipid nanoparticles (SLN) for controlled drug delivery:a review of the state of the art. Eur J Pharm Biopharm. 2000;50:161-177.
41. Teixeira M, Alonso MJ, Pinto MMM, Barboso CM. Development and characterization of PLGA nanospheres and nanocapsules containing xanthone and 3-methoxyxanthone. Eur J Pharm Biopharm. 2005;59:491-500.
42. Dillen K, Weyenberg W, Vandervoort J, Ludwig A. The influence of the use of viscosifying agents as dispersion media on the drug release properties from PLGA nanoparticles. Eur J Pharm Biopharm.2004;58:539-549.
43. Mitra A, Lin S. Effect of surfactant on fabrication and characterization of paclitaxel-loaded polybutylcyanocrylate nanoparticulate delivery systems. J Pharm Pharmacol. 2003;55:895-902.
44. Wiśniewska M. The temperature effect on electro kinetic properties of the silica–polyvinyl alcohol (PVA) system. Colloid Polym Sci.2011;289:341-344.
45. Ye J, Wang Q, Zhoua X, Zhang N. Injectable loaded solid lipid nanoparticles as passive targeting therapeutic agents for rheumatoid arthritis. Int J Pharm. 2008;352:273-279.
46. Derakhshandeh K, Erfan M, Dadashzadeh S. Encapsulation of 9- nitrocamptothecin, a novel anticancer drug, in biodegradable nanoparticles: factorial design, characterization and release kinetics. Eur J Pharm Biopharm. 2007;66:34-41.
47. Shah M, Pathak K. Development and statistical optimization of solid lipid nanoparticles of simvastatin by using 2 3 full-factorial design. AAPS Pharm Sci Tech. 2010;78:1-8.
48. Yang Y, Chung T, Bai X, Chan W. Effect of preparation conditions on morphology and release profiles of biodegradable polymeric microspheres containing protein fabricated by double-emulsion method. Chem Eng Sci. 2000;55:2223-2236.
49. Reddy LH, Vivek K, Bakshi N, Murthy RS. Tamoxifen citrate loaded solid lipid nanoparticles (SLN): preparation, characterization, in vitro drug release, and pharmacokinetic evaluation. Pharm Dev Technol. 2006;11:167-177.
50. Barzegar-Jalali M. A model for linearizing drug dissolution data. Int J Pharm. 1990;63:6-11.
51. Xiong XY, Tam KC, Gan LH. Release kinetics of hydrophobic and hydrophilic model drugs from pluronic F127/poly(lactic acid) nanoparticles. J Control Release. 2005;103:73-82.
52. Siemann J, Peppas NA. Modeling of drug release from delivery systems based on hydroxypropylmethylcellulose (HPMC). Adv Drug Deliv Rev. 2001;98:139-157.
53. Li Z, Chen P, Xu X, Ye X, Wang J. Preparation of chitosan-sodium alginate microcapsules containing Zns nanoparticles and its effect on the drug release. Mater Sci Eng C. 2009;29:2250-2253.
54. Mainardes RM, Evangelista RC. PLGA nanoparticles containing praziquantel: effect of formulation variables on size distribution. Int J Pharm. 2005;290:137-144.
55. Venkateswarlu V, Manjunath K. Preparation characterization and in vitro release kinetics of clozapine solid lipid nanoparticles. J Control Rel. 2004;95:627-638.
56. Kumara VV, Chandrasekar D, Ramakrishna S, Kishan V, Raoa YM, Diwan PV. Development and evaluation of nitrendipine loaded solid lipid nanoparticles: Influence of wax and glyceride lipids on plasma pharmacokinetics. Int J Pharm. 2007;335:167-175.
57. Malzert-Freon A, Vrignaud S, Saulnier P, Lisowski V, Benoit JP, Rault S. Formulation of sustained release nanoparticles loaded with a tripentone, a new anticancer agent. Int J Pharm. 2006;320:157-164.
58. Jiang B, Hu L, Gao C, Shen J. Ibuprofen-loaded nanoparticles prepared by a co- precipitation method and their release properties. Int J Pharm. 2005;304:220-230.
59. Muller RH, Schwarz C, Mehnert W, Muhlen AZ. Incorporation of lipophilic drugs and drug release profiles of solid lipid nanoparticle. Bioact Mater Contr Rel Soc Inc. 2000;21:88-95.
60. Annette ZM, Cora S, Wolfgang M. Solid lipid nanoparticles (SLN) for controlled drug delivery and release mechanism. Eur J Pharm Biopharm. 1998;45:149-155.
61. Sham JOH, Zhang Y, Finlay WH, Roaa WH, Lobenberg R. Formulation and characterization of spray-dried powders containing nanoparticles for aerosol delivery to the lung. Int J Pharm. 2004;269:457–467.
62. Grenha A, Seijo B, Serra C, Lopez CR. Chitosan nanoparticle-loaded mannitol microspheres: structure and surface characterization. Biomacromolecules. 2007;8:2072–2079.
63. Grenha A, Lopez CR, ELS C, Seijo B. Microspheres containing lipid/chitosan nanoparticles complexes for pulmonary delivery of therapeutic proteins. Eur J Phar Biopharm. 2008;69:83–93.